environmental microbiology

Environmental Microbiology (2020) **22**(11), 4633–4646 doi:10.1111/1462-2920.15206

Differential distribution and proteomic response of *Saccharomyces cerevisiae* and non-model yeast species to zinc

Beatriz García-Béjar,[1*] **Rebecca A. Owens**,[2*] **Ana Briones**[1] **and María Arévalo-Villena**[1]

[1]*Department of Analytical Chemistry and Food Technology, University of Castilla-La Mancha, Ciudad Real, 13071, Spain.*

[2]*Department of Biology, Maynooth University, Maynooth, Co. Kildare, Ireland.*

Summary

Zinc surplus in yeast cells has been previously investigated thanks to transcriptomic studies by using traditionally *Saccharomyces cerevisiae* as a model. However, proteome response under zinc-replete conditions needs to be further studied in yeast. For that reason, eight yeast strains from seven different species were inoculated in zinc-depleted and zinc-replete media. The quantitative and qualitative comparative label-free proteomic analysis enabled the identification of between 2000 and 3000 proteins from each strain, and changes to the proteome ranged from 2.5% to 43.7% of identified proteins. Functional analysis (Blast2Go) has allowed the characterization of differentially abundant proteins. Common zinc-responsive proteins have been detected for the eight strains such as oxidoreductases and transferases (increased in abundance) although more of the changes detected were not shared by all the strains tested. Zinc distribution under replete conditions has been analysed in cell wall fractions, and cytoplasm plus organelles (intracellular fraction), with the latter identified to be the main zinc reservoir. Additionally, the energy dispersive spectroscopy coupled to the scanning electron microscopy technique has permitted the visualization of zinc in the whole cell. Proteomic analysis revealed that while there were some shared responses, the non-model yeast species also showed distinct proteomic profiles in zinc-replete conditions, compared to *S. cerevisiae*, revealing new zinc-responsive proteins in yeast.

Received 18 June, 2020; accepted 18 August, 2020. *For correspondence. E-mail beatriz.gbermejo@uclm.es; Tel: +353 1 708 3839; Fax: +353 1 708 3845. E-mail rebecca.owens@mu.ie.

Introduction

Heavy metals are naturally occurring elements but, due to human industrial activity, their concentrations have increased seriously in the environment, disrupting their balance (Tchounwou *et al*., 2012). Also, these elements are toxic at low concentrations and tend to accumulate in water and the food chain where they can produce damage to living organisms (Ayangbenro and Babalola, 2017). Nevertheless, in appropriate concentrations these metals are essential for the biological function of cells, such as structural or enzyme cofactors, or as part of various oxidation–reduction reactions (Tchounwou *et al*., 2012).

Zinc is a heavy metal and an important micronutrient involved in the growth, physiology and metabolism of yeasts. The concentration of zinc must be controlled in a suitable range, which has been estimated between 0.1 and 0.5 mM in intracellular concentrations (Eide, 2006; Zhao and Bai, 2012). In normal growing conditions, the majority of intracellular zinc is bound in high-affinity sites on proteins. In addition, it is known that DNA, lipids and small molecular weight compounds, such as amino acids, organic anions and glutathione may have low-affinity zinc-binding sites (Eide, 2006).

Genomic and transcriptomic studies have allowed the identification of some proteins involved in zinc binding, expanding our understanding of zinc homeostasis using *Saccharomyces cerevisiae* as a model. Moreover, recent studies have indicated that this microorganism could have a total of 582 proteins with zinc-binding domains encoded within the genome, with proteomic detection of 229 of these candidates under zinc-replete conditions (Wang *et al*., 2018).

Although proteomes of non-*Saccharomyces* yeasts have not been deeply studied, *S. cerevisiae* has given valuable information about proteins that bind zinc ions. For example, Adh1 alcohol dehydrogenase, SOD1 superoxide dismutase (SOD), Fba1 aldolase and several zinc-binding ribosomal subunits have been predicted as proteins with a high number of bound zinc ions. In fact, high abundance zinc-binding proteins accounted for almost 90% of the total zinc requirement of the cell

(Wang *et al*., 2018). This ion also can be a structural component of certain proteins such as in the case of zinc finger proteins (Zfp), which have been characterized in the ribosome and carry out an important role in transcriptional regulation of cellular metabolism (Ghaemmaghami *et al*., 2003; MacPherson *et al*., 2006).

In general, in media with surplus zinc, cells tend to use two principal ways to maintain homeostasis. The ion can be excluded from the inner parts of the cells to the exterior by using membrane transporters or can be stored in the organelles (Regalla and Lyons, 2005).

Zinc homeostasis in *S*. *cerevisiae* is regulated mainly by the transcription factor Zap1, with Zap1 homologues characterized in other non-*Saccharomyces* yeast like *Candida albicans* (Wilson and Bird, 2016). Zap1 can activate its own transcription increasing the gene expression and the Zap1 proteins levels under zinc-limiting conditions (Eide, 2009). In these conditions, transporters from the ZIP family (Zrt-, Irt-like Protein), which have been identified in *S*. *cerevisiae*, transport zinc or other metal ions from the extracellular space into the cytoplasm, with different transporters (Zrt1 and Zrt2) responsible for zinc uptake, as well as Fet4 that facilitates zinc transport to cytoplasm although it is not a member of ZIP family (Chung and Bird, 2019). Once the ion is inside the cell, it can be transported to the endoplasmic reticulum or the Golgi apparatus by the Msc2/Zrg17 complex, although in high concentrations the expression of Zrg17 can be suppressed (Ellis *et al*., 2005). However, the yeast's major site of zinc accumulation is the vacuole and is regulated by two proteins from the cation diffusion facilitator (CDF) family (Eide, 2006) but, under zinc-replete conditions, this storage capability could be limited (Simm *et al*., 2007). Although zinc efflux transporters are known in some eukaryotic and prokaryotic cells, a lack of information is found in yeast.

Therefore, the purpose of the investigation was to study the proteome response under zinc-replete conditions in one *Saccharomyces* strain and seven non-*Saccharomyces* strains in order to get more information about proteins involved. This response was compared with strains grown in zinc depleted conditions to help better understand zinc homeostasis as well as survey the processes associated with survival in low zinc concentrations. Additionally, the distribution of zinc in cells was analysed to profile the accumulation of this metal ion in each strain.

Materials and methods

Yeast strains

Strains from *Saccharomyces* and non-*Saccharomyces* species were chosen due to their zinc bioremediation properties and tolerance based on previous assays (García-Béjar *et al*., 2020): *Candida parapsilosis* (ECF42), *Wickerhamiella sorbophila* (ECF12), *Candida tropicalis* (AK11), *Diutina rugosa* (FR19 and ECF61), *Rhodotorula mucilaginosa* (EB39) and *Saccharomyces cerevisiae* (EB83) as well as one strain from *Aureobasidium pullulans* (FH1) in the yeast-like form. These strains are deposited in the public yeast collection of the University of Castilla—La Mancha (Spain) and were isolated from different environments of this Spanish area such as flowers, birds and food industry air (Supplementary Table 1).

All strains were grown in 5 ml of YPD broth (yeast extract 10 g/L; glucose 20 g/L; peptone 20 g/L) for 24 h at 30°C with slight shaking conditions (150 rpm). Cells were cultured on YPD agar (yeast extract 10 g/L; glucose 20 g/L; peptone 20 g/L; agar 20 g/L) and grown at 30°C, 24 h. Plates with isolated colonies were kept at 4°C until required.

Proteomic analysis

Culture conditions. Before protein extraction, yeast strains were inoculated in 5 ml of YPD and incubated for 24 h at 30°C with slight stirring (150 rpm). Strains were labelled as either 'Zinc depleted' or as 'Zinc replete' and each labelled sample was grown in triplicate. Overnight cultures were centrifuged at 1000*g* for 5 min at 4°C, then pellets were collected aseptically and washed with sterile deionized water. Washed pellets were inoculated in 50 ml sterile flasks with 25 ml of MSM + Glu (Glucose 10 g, K_2HPO_4 0.4 g, KH_2PO_4 0.2 g, NaCl 0.1 g, $MgSO_4.7H_2O$ 0.5 g, $MnCl_2$ 0.01 g, $Fe(SO_4)_3$ 0.01 g and Na_2MoO_4 0.01 g per litre) adjusted to pH 7. These samples could contain trace amounts of contaminating zinc from glassware or media reagents, so are referred to as zinc-depleted samples rather than zinc free. Zinc replete samples were prepared by supplementing with Zn^{2+} at a final concentration of 25 mg/L of Zn^{2+} (382 μM; Zn-replete conditions), using a 100× concentrated $ZnSO_4{\cdot}7H_2O$ stock solution. Cultures were incubated at 30°C for 24 h at 150 rpm.

Subsequently, zinc depleted, and zinc-replete cultures were both collected at the end of their growth cycle (stationary phase) and centrifuged (1000*g*, 5 min, 4°C), pellets were washed with ice-cold PBS and centrifuged again in the same conditions. Collected pellets were frozen with liquid nitrogen and all samples were kept at −80°C until protein extraction.

Protein extraction, digestion and cleaning. Protein extraction was performed using an adaptation of the protocol described by Saleh *et al*. (2018). Briefly, cell pellets were re-suspended in cold lysis buffer (100 mM Tris–HCl, 50 mM NaCl, 20 mM EDTA, 10% Glycerol, 1 mM phenylmethylsulfonyl fluoride (PMSF), 1 μg ml^{-1} Pepstatin

pH 7.5) and sonicated using an MS73 tip (Bandelin SONOPULS) for 10 s × 3, at 20% power, followed by incubation on ice for 1 h. Protein concentration was determined by the Bradford assay and total cell lysates were adjusted to 0.25 mg/ml with 50 mM ammonium bicarbonate (Merck), followed by reduction with a final concentration of 5 mM dithiothreitol for 20 min at 56°C. Samples were allowed to cool and alkylated with excess iodoacetamide (15 mM final), in the dark for 15 min. Proteins were then trypsin (Promega) digested overnight at 37°C in the presence of ProteaseMax (Promega) and digestion was stopped by the addition of trifluoroacetic acid to a final concentration of 1% (v/v). Acidified samples were centrifuged 12 000*g* for 10 min at room temperature and supernatants were dried in a miVac centrifugal concentrator (GeneVac) at 30°C for approximately 3 h. Samples were cleaned-up for Q-Exactive analysis using C18 Zip-Tips (ThermoFisher). Finally, cleaned products were dried again in SpeedyVac at 30°C for approximately 1 h and kept at −20°C until analysis.

Proteome analysis by Q-Exactive mass spectrometer. A quantity of digested peptides (0.75 μg) were analysed from each sample using a ThermoFisher Q-Exactive mass spectrometer, with online peptide separation though a Dionex 3000 RSLCnano equipped with an Easy-Spray PepMap™ column (50 cm × 75 μm, 2 μm particles). Peptides were separated on a 90 min gradient (10%–40% Solvent B; A: 0.1% (v/v) formic acid in 3% (v/v) acetonitrile, B: 0.1% (v/v) formic acid in 80% (v/v) acetonitrile). MS detection was carried out at a resolution of 70 000, with a Top15 method used for MS/MS scans (Collins *et al*., 2017).

Bioinformatic analysis. Quantitative proteomics and data analysis were performed using MaxQuant software (Version 1.6.2.10; https://www.maxquant.org/maxquant/) (Cox and Mann, 2008), with the Label Free Quantification algorithm used to generate normalized spectral intensities and infer relative protein abundance (Luber *et al*., 2010). Protein databases used for searches were downloaded from www.uniprot.org (January 2019) or were obtained from https://www.ncbi.nlm.nih.gov/ (*D. rugosa*, November 2019). If a protein database from the same species was not available, the database from a related species was used (Supplementary Table 1). Additionally, Perseus software (Version 1.6.2.3; https://maxquant.net/perseus/) was used to organize the data and perform statistical analysis (Tyanova *et al*., 2016). Those proteins that matched to a reverse database or contaminants database, only identified by site and that were only identified by a single peptide were removed. Proteins were further filtered, retaining only proteins that were detected in at least two replicates from at least one group (zinc depleted or zinc replete samples) (Delgado *et al*., 2019). Quantitative analysis was performed using a two-samples test to compare zinc replete samples to the zinc-depleted condition. Quantitative results included proteins with a significant abundance change (fold change ≥2, $p < 0.05$) between the tested conditions. Qualitative results included proteins that were detected in at least two replicates of either the zinc depleted or the zinc replete sample but were undetectable in the comparison sample. Quantitative and qualitative results were combined for functional analysis and collectively referred to as differentially abundant proteins (DAPs).

Blast2GO software (https://www.blast2go.com/) was used for the functional analysis of identified proteins, performing a gene ontology (GO) term enrichment analysis using a Fisher's exact test. Significantly enriched GO terms ($p < 0.05$) were identified for proteins altered in abundance in the zinc-replete conditions compared to the total reference proteome.

In the case of products of Zap1-regulated genes from *S. cerevisiae*, the database OrthoDB v10.1 (https://www.orthodb.org/) was used to identify orthologues in the non-*Saccharomyces* strains studied (Kriventseva *et al*., 2018; Wang *et al*., 2018).

Zinc distribution in yeast cells

Zinc distribution in the yeast strains was analysed using two different methods. The analysis of zinc distribution in the whole cell was performed using the energy dispersive spectroscopy coupled to the scanning electron microscopy (SEM-EDS) together with the quantification and distribution of zinc in the supernatant, in the intracellular fraction and bounded on the cell wall that was carried out by voltammetric measurements.

SEM-EDS for zinc distribution in the whole cell. Samples were prepared for analysis as follows. Fresh cultures grown overnight in YPD were collected by centrifugation (1000*g*/5 min/4°C) and the whole pellet was inoculated in 500 ml sterile flasks with 250 ml of MSM + Glu supplemented with 25 mg/L of zinc and incubated at 30°C (24 h, 200 rpm). After this time, cells were recovered by centrifugation, washed twice with dH_2O and dried at 60°C for approximately 5 h.

Dried samples were introduced on the SEM and were radiated with X-rays, and X-rays emitted by different points of the sample were detected by the EDS. Since the scattered energy of X-rays is specific of each chemical element, it was possible to carry out a qualitative and quantitative EDS microanalysis.

Voltammetric measurements of zinc in the cell wall and intracellular fraction. First, cells were grown in MSM + Glu

supplied with 25 mg/L of zinc at 30°C (200 rpm) at initial cell counts of 10^6 cells ml^{-1}, using the same conditions as described previously in the 'Culture conditions' section. The experiment was carried in triplicate and only cells under Zn-replete conditions (+Zn) were analysed.

In order to determine how much zinc was associated with each cell, cell viability was analysed by doing plate counts on YPD agar using a spiral plater (Eddy Jet 2, IUL Instruments, Barcelona, Spain). Plates were incubated at 30°C for 2 days and colonies were counted with an automatic counter (Flash & Go, IUL Instruments).

For zinc analysis, supernatant (MSM + Glu with residual zinc) and cells were separated by centrifugation (1000*g*, 5 min, 4°C). Supernatants were kept at 4°C until needed and pellets were washed twice with cold saline solution (0.9%) and re-suspended in PBS.

Cell disruption was done by the addition of acid-washed glass beads (212–300 μm, Sigma–Aldrich, Steinheim, Germany) to cell suspension in 2 ml tubes. Cells were then agitated at high speed by vortex mixing 10 times for 30 s each, keeping the samples on ice for 5 s between agitation steps. Cell disruption was verified by optical microscopy observation. Cell walls and glass beads were collected by centrifugation (1000*g*, 5 min, 4°C), intracellular content was transferred to a new 1.5 ml tube and cell walls were washed twice with cold saline solution. Once cell walls were ready for digestion, a 30% nitric acid solution was added, and samples were mixed for 30 s in a vortex mixer. When the digestion was done, glass beads were recovered by centrifugation in the same conditions described ahead and extracted zinc from the cell wall was transferred to a new 1.5 ml tube.

Zinc analysis from the supernatant, intracellular fraction and cell wall was carried out by instrumentation voltammetric measurements, which were performed with a Metrohm Computrace voltammetric analyser potentiostat (model 757 VA, Eco-Chemie, Utrecht, Netherlands). A conventional three-electrode system consisting of Ag/AgCl/KCl reference electrode, a hanging mercury drop electrode as a working electrode, and a platinum rod as an auxiliary electrode was used. The whole measurements were automated and controlled through the programming capacity of the apparatus. The data were treated through a PC connected to the electrochemical analyser 757 VA Computrace.

Results

Proteome analysis

Analysis by Q-Exactive mass spectrometer and identification by the bioinformatics programs permitted the survey of the proteomes of certain *Saccharomyces* and non-*Saccharomyces* strains. Moreover, quantitative ($p < 0.05$; fold change ≥2) and qualitative (unique to zinc replete or zinc depleted conditions) changes in proteins between zinc replete (+Zn) and the zinc-depleted samples (−Zn) were analysed in all the strains (Table 1; Supplementary Table 2). In general, the number of proteins identified from each species ranged between 2000 and 3000. The highest number of proteins ($n = 2907$) were detected in FH1 (*A. pullulans*) strain and the lowest (n = 2281) in EB83 (*S. cerevisiae*) strain.

Yeast proteome response to zinc-replete conditions turned out to be different for each strain, with all of the changes in the proteome summarized in Table 1. *Candida tropicalis*. strain (AK11) showed the highest changes to the proteome due to zinc presence; quantitative and qualitative comparison revealed that 600 proteins increased in abundance and 502 decreased in abundance (43.7% of the total proteome analysed) between zinc replete and zinc-depleted samples. Within the species from the *Candida* genus, there was a disparity in the level of proteome changes observed in response to zinc treatment. In contrast to *C. tropicalis* (AK11), protein abundance changes in *C. parapsilosis* (ECF42) and *W. sorbophila* (ECF12) were minimal (2.5% and 4.3% in their total proteome respectively), so zinc at this concentration (382 μM) has a limited action on the proteome of these yeasts (Pearson's correlation (*r*) compared to the control: 0.97–0.99 in ECF42 and 0.96–0.99 in ECF12). Hierarchical clustering revealed that within each strain tested, replicates clustered based on the zinc condition (+Zn/−Zn), with the exception of *C. parapsilosis* which

Table 1. Proteins with altered abundance in the different yeast strains inoculated in zinc-replete conditions.

Strain	Total proteins	Up in treatment	Down in treatment	Unique to treatment	Unique in control
FH1 (*A. pullulans*)	2907	99	113	68	169
ECF42 (*C. parapsilosis*)	2342	2	1	8	47
ECF12 (*C. sorbophila*)	2471	38	8	31	30
AK11 (*C. tropicalis*)	2518	284	334	316	168
FR19 (*D. rugosa*)	2469	198	256	185	66
ECF61 (*D. rugosa*)	2449	236	307	263	72
EB39 (*Rh. mucilaginosa*)	2580	219	205	173	72
EB83 (*S. cerevisiae*)	2281	163	222	84	218

showed limited proteomic differentiation in response to changing zinc concentrations (Fig. 1). In the case of *W. sorbophila* strain, hierarchical clustering did show distinct grouping of the zinc replete and depleted samples, however, these differences in the proteome were minimal when considering only proteins with a fold change ≥2 ($p < 0.05$). It is evident that exists a change in the proteome in most of the strains although it is necessary to

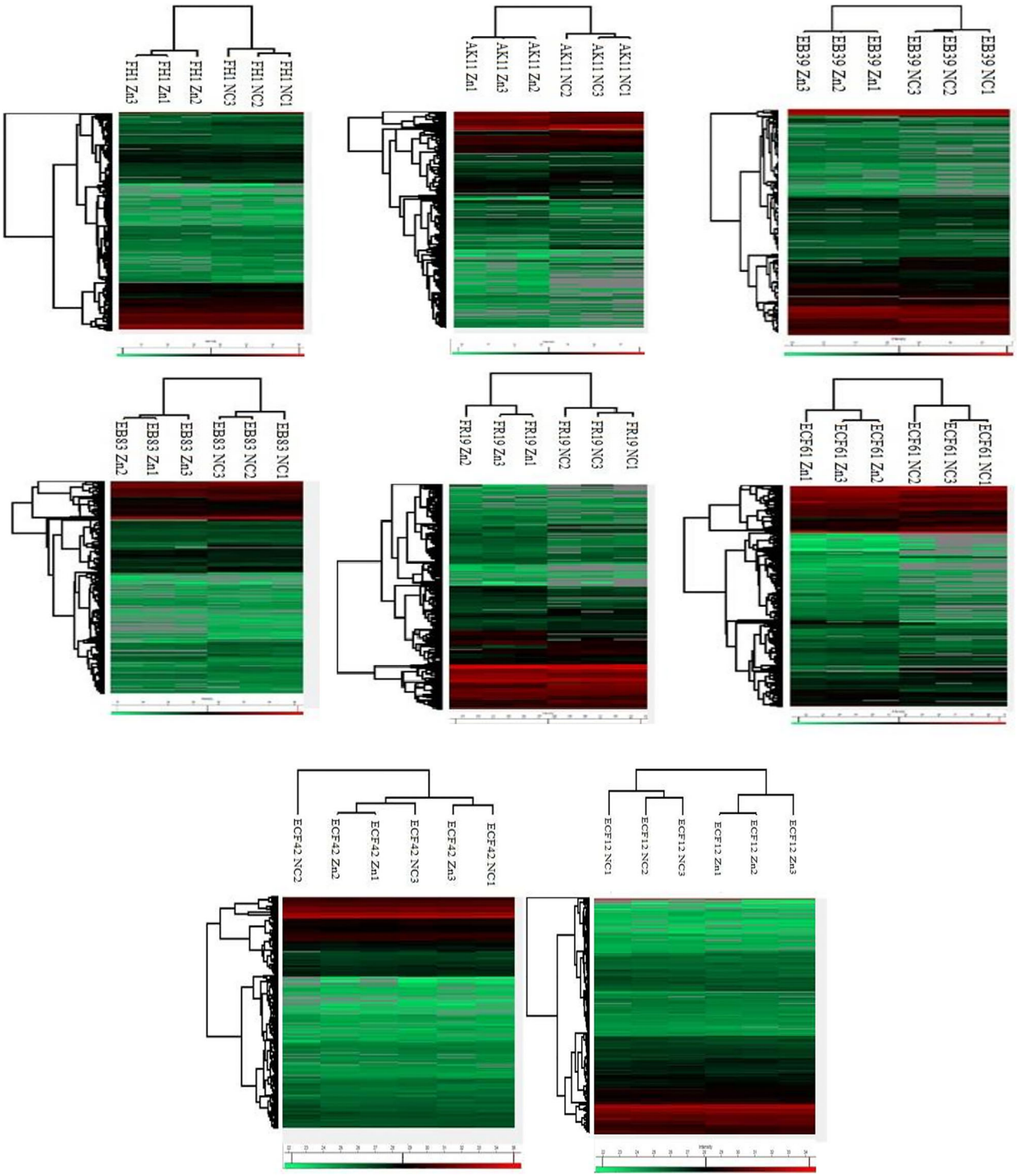

Fig. 1. Heat map showing the hierarchical clustering from label-free quantitative data for the zinc-depleted sample (NC) and treated sample (Zn) for each strain. [Color figure can be viewed at wileyonlinelibrary.com]

verify if this change is a response to treatment or could be due to the diverse zinc homeostasis pathways of the strains based on the quantitative analysis.

GO term enrichment, based on Blast2GO analysis, was observed for proteins altered in abundance in the zinc replete compared to zinc-depleted samples. Functional enrichment analysis allowed us to determine distinct functional profiles for each strain's proteome under zinc-replete conditions (Supplementary Table 3). In general, zinc-associated alterations to the proteome were different across each of the strains based on GO terms, although some common changes were detected.

Among the proteins that were commonly elevated in abundance in each strain (Fig. 2), only structural constituent of the ribosome proteins, enzymes with oxidoreductase and transferase activities were significantly enriched in zinc-replete conditions in comparison with zinc-depleted samples ($p < 0.05$). ATPases were also significantly enriched in this cohort of DAPs in most of the strains ($p < 0.05$), except in EB39 (*Rh. mucilaginosa*) and EB83 (*S. cerevisiae*). Additionally, enzymes involved in the tricarboxylic acid cycle significantly increased in abundance ($p < 0.05$), specifically in *C. tropicalis* (AK11) and *D. rugosa* (FR19) strains. While some enzymes requiring a metal ion co-factor were elevated in response to zinc treatment, only one metal ion binding GO term (copper ion binding) was significantly enriched ($p < 0.02$) in one of the strains (*A. pullulans*—FH1). Additionally, in both *D. rugosa* strains (FR19 and ECF61) there was an increment on the number of proteins related with iron ion transport ($p < 0.04$) and, in ECF61, there was also an increase in proteins related with cellular response to iron ion starvation ($p < 0.008$). RNA-binding proteins were elevated in response to zinc presence in most of the strains except in *A. pullulans* (FH1) and *D. rugosa* (ECF61), in addition to structural constituents of the ribosome, with between 11 and 70 subunits elevated in all strains ($p < 0.04$). Proteins associated with the mitochondria structure ($p < 0.05$) or mitochondrial ribosomes ($p < 0.05$) increased in abundance in all samples, with the exception of *A. pullulans* (FH1). Proteins associated with the Golgi apparatus membrane were significantly elevated in abundance in EB83 (*S. cerevisiae*) strain as well. Lastly, there was a significant increment ($p < 0.05$) in integral membrane proteins of FH1 (*A. pullulans*) and AK11 (*C. tropicalis*) strains in response to zinc.

Functional enrichment analysis of proteins that decreased in abundance in response to zinc (Fig. 3) revealed proteins related with ion transmembrane transporter activity ($p < 0.05$) and specific metal ion binding ($p < 0.05$), in strains FH1 (*A. pullulans*) and AK11 (*C. tropicalis*). Proteins with metal ion transmembrane transporter activity were significantly lower following zinc treatment in *C. tropicalis* strain (AK11) along with calcium ion binding proteins ($n = 6$; $p < 0.05$) (Supplementary Table 3). Moreover,

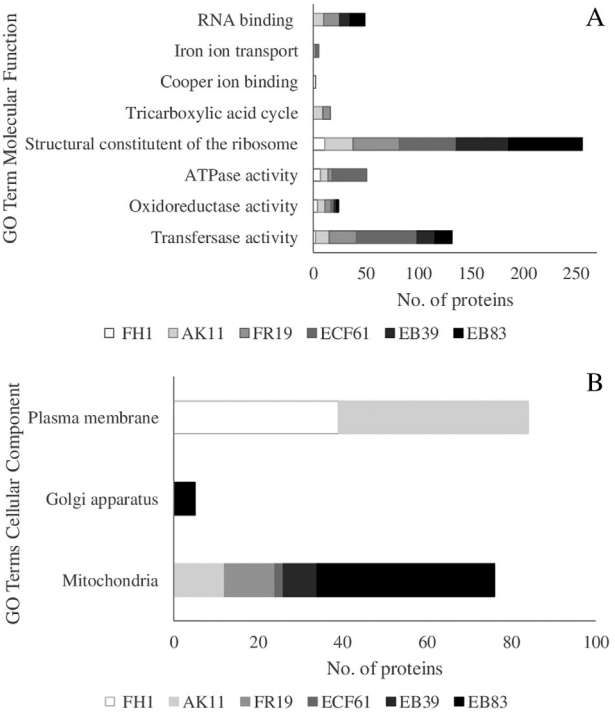

Fig. 2. Principal GO terms associated with the molecular function (A) and cellular component (B) of proteins elevated in abundance in zinc replete.

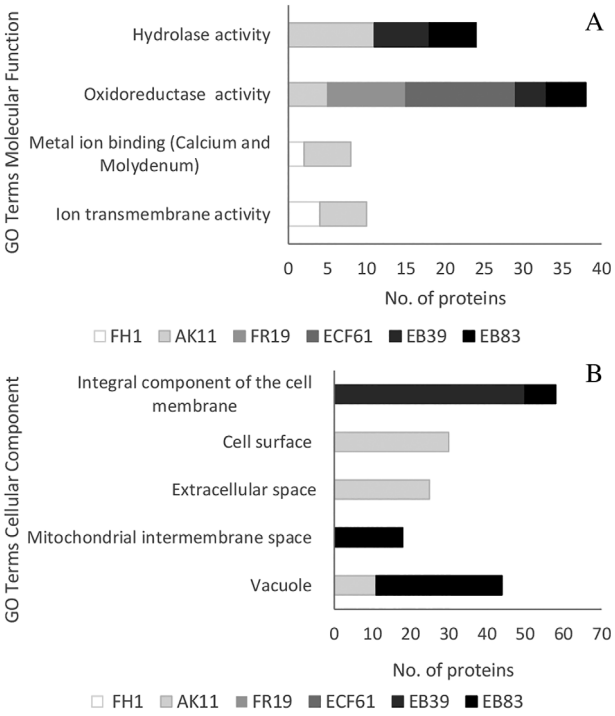

Fig. 3. Principal GO terms associated with the molecular function (A) and cellular component (B) of proteins decreased in abundance.

there was a significant ($p < 0.05$) decrease in specific oxidoreductases (cytochrome-c oxidase, catalase-peroxidase, dehydrogenase) in all strains except *A. pullulans* (FH1). Enrichment analysis also revealed a reduction in the number of proteins with hydrolase activity ($p < 0.05$) in AK11 (*C. tropicalis*), EB39 (*Rh. mucilaginosa*) and EB83 (*S. cerevisiae*) strains. Vacuole-associated proteins (membrane and lumen) decreased in abundance significantly ($p < 0.01$) in *C. tropicalis* (AK11) and in *S. cerevisiae* (EB83) strains. Also, in *S. cerevisiae*, there was a significant reduction in proteins from the mitochondrial intermembrane space ($n = 18$) and integral components of the plasma membrane ($n = 8$). Proteins associated with the extracellular region ($n = 30$) and the cell surface ($n = 25$) in *C. tropicalis* (AK11) were decreased in abundance ($p < 0.05$), as well as proteins characterized as integral components of the membrane ($n = 50$) from *Rh. mucilaginosa* (EB39) strain.

Metal ion binding proteins. A number of putative metal ion binding proteins were altered in abundance under zinc-replete conditions (Table 2), and this analysis revealed that the highest number of differentially abundant metal ion binding proteins were found in AK11 (*C. tropicalis*) and the lowest in ECF42 (*C. parapsilosis*). Most of the proteins with active metal ion binding sites (Supplementary Table 4) were associated with oxidation–reduction processes, including cytochrome C and b5, proteins P450, P450 61 and P450 52A11 (A0A074X5I5, KAA8901173.1, ACN87252.1, KAA8901173.1, KAA 8903790.1, KAA8903790.1, A0A109FLY8, A0A2T0FJN2, C5MAM3), SOD (A0A074XI36, A0A367YK97, C5MEF5, C5MA54, C5MIY4, A0A109FM53), alcohol dehydrogenase (A0A367Y9M8, C5M8S5, KAA8905622.1, KAA 8906565.1), hydroxylases (C5M796, C5MI42, P41735, P47120), ketol-acid reductoisomerases (C5M977, KAA 8897139.1), sterol 14-alpha-demethylase (KAA8905632.1), monooxygenase (KAA8907714.1) and NADP-dependant malic enzyme (A0A074Y8L1, P36013). However, some oxidation–reduction proteins were decreased in abundance following zinc addition, with most of them part of the dioxygenase (A0A074XT47, A0A074X1E9, A0A 074XLG3, C5M2N8, A0A120E6A9, KAA8896736.1) and dehydrogenase family (A0A074X7I1, A0A074X9E9, A0A 074YIX8, A0A074XLP8, A0A074XS02, A0A074XS11, C5M5Y2, C5MC37, C5MC43, KAA8902437.1, KAA 8903461.1, A0A120E6L0, A0A120E7W1). Additionally, different metallopeptidases were altered in abundance (Supplementary Table 4) in some strains, which were elevated significantly ($p < 0.05$) in zinc replete samples, excluding EB39 strain (*Rh. mucilaginosa*). These proteins were mainly associated with the mitochondrial intermembrane space, inner membrane and matrix (C5M5K4, C5MEL8, C5MGT6, C5M9D1, C5MGC9, KAA8902973.1, KAA8905642.1, KAA8899097.1, A0A120E8Z0, A0A 2S5B279, P10507, P11914, P32898).

Table 2. Metal and zinc ion binding proteins with altered abundance.

	Metal ion binding	
Strain	Up + unique in Zn replete	Down in treatment + Zn deplete
FH1 (*A. pullulans*)	17	27
ECF42 (*C. parapsilosis*)	2	7
ECF12 (*C. sorbophila*)	7	3
AK11 (*C. tropicalis*)	62	50
FR19 (*D. rugosa*)	21	16
ECF61 (*D. rugosa*)	40	19
EB39 (*Rh. mucilaginosa*)	45	30
EB83 (*S. cerevisiae*)	27	16

Zap1-regulated proteins. Saccharomyces cerevisiae. Zap1-regulated proteins ($n = 16$) that had previously shown an abundance change ($p < 0.05$, Log2FC ≥ 2) in response to zinc (Wang *et al*., 2018) were surveyed in our data. Of these, 16 proteins were detected in EB83 (*S. cerevisiae*) proteomics in this study. According to Wang *et al*. (2018), 18 of these proteins were present at a lower abundance in zinc replete compared to zinc-depleted conditions across a range of timepoints. This study mirrors these zinc-related changes in *S. cerevisiae* EB83, with 10 of these proteins also observed to decrease in abundance following zinc addition (Supplementary Table 5), thus validating the experimental method. Orthologues of these Zap1-regulated proteins were identified in each of the strains tested, to determine if similar responses are shown in the non-*Saccharomyces* strains evaluated (Fig. 4; Supplementary Table 5). Orthologues of some of these proteins were identified in all strains, although no changes in abundance were detected in *C. parapsilosis* (ECF42) and *W. sorbophila* (ECF12) for these proteins. From the Zap1-regulated proteins, an orthologue was detected in at least one of the non-*Saccharomyces* species for 18 proteins. Several *S. cerevisiae* (EB83) Zap1-regulated proteins ($n = 10$) were significantly lower in abundance in Zn+ conditions, in line with results observed by Wang *et al*. (2018). These included the 12 kDa heat shock protein HSP12, which was also at a lower abundance in *D. rugosa* (FR19 and ECF61) and *C. tropicalis* (AK11) and the vacuolar proteases saccharopepsin Pep4, at reduced abundance in *D. rugosa* ECF61 and *Rh. mucilaginosa* EB39, and cerevisin Prb1, reduced in *A. pullulans* FHI, *Rh. mucilaginosa* EB39 and *C. tropicalis* AK11, in response to Zn+ conditions. In some cases, orthologous proteins showed opposing alteration in abundance in non-Saccharomyces species in response to zinc, including carboxypeptidase Y Prc1 (increased in *C. tropicalis* AK11), mitochondrial cysteine

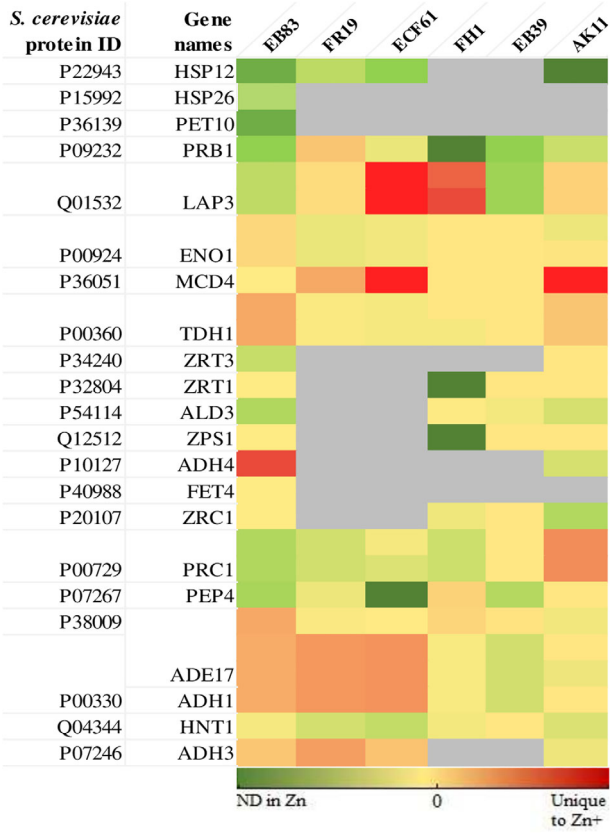

Fig. 4. Abundance change of Zap1-regulated zinc responsive *S. cerevisiae* proteins and their orthologues found in the non-Saccharomyces strains tested. Green gradients represent proteins with decreased abundance in Zn+ compared to Zn− samples, orange/red gradients indicate proteins with increased abundance in Zn+ compared to Zn− samples and yellow gradients show proteins with no significant differences. When an orthologue was not found it was represented in grey. [Color figure can be viewed at wileyonlinelibrary.com]

protease 1 Lap3 (increased in *D. rugosa* ECF61, *A. pullulans* FH1) and GPI ethanolamine phosphate transferase 1 Mcd4 (increased in *D. rugosa* ECF61, *C. tropicalis* AK11) (Supplementary Table 5). It was noticed that the smallest number *S. cerevisiae* Zap-1 regulated orthologues were detected in *D. rugosa* strains (ECF61 and FR19) compared to the other strains tested. Moreover, the strains that presented the most similar Zap1-regulated protein abundance profile to *S. cerevisiae* (EB83) were *Rh. mucilaginosa* (EB39) and *D. rugosa* (FR19), with *A. pullulans* (FH1) showing more opposing abundance changes (Fig. 4). This could point to differences in the homeostasis mechanisms carried out in these different yeast species, although further investigation would be required to confirm this. Moreover, these results suggest that Zn homeostasis mechanisms are closely related to the change on the proteome produced by Zn+ conditions in the yeast strains studied.

Zinc distribution in yeast cells

Visualization of zinc distribution in yeast cells by SEM-EDS. After incubation in zinc-replete and zinc-depleted media and a drying process of the biomass, the samples were introduced on the SEM, radiated with X-rays and the signals generated by the chemical compounds were captured by EDS.

First, as expected, no zinc signal was recorded from negative controls, although compounds such as carbon, oxygen, sodium and chlorine were identified. It was also observed that cells treated with zinc (+Zn) were affected after incubation, and different ion distributions were found depending on the strains. SEM-EDS image can be observed for *S. cerevisiae* (EB83) as an example (Fig. 5), with the remaining SEM-EDS images included in Supplementary Fig. 1.

It was noticed that most concentrated zinc signals were observed in strains ECF42 (*C. parapsilosis*), AK11 (*C. tropicalis*), ECF61 (*D. rugosa*) and EB39 (*Rh. mucilaginosa*) while in the rest of the samples the zinc signal was more homogeneously distributed. As can be observed, damaged cells presented strong zinc signals in the contiguous areas where the cell wall has been broken (e.g. FH1 and EB83) which could indicate its intracellular location and its liberation to the extracellular space. In fact, the ion signal was detected in the whole cell that was undamaged (e.g. AK11 and ECF61). Although distribution in the different cell parts or organelles could not be quantified using this technique, proteomic results supported the fact that a cell stress response existed and the major changes have been associated with certain organelles or inner enzymes, as well as, metal ion transporters that have decreased, pointing to zinc saturation of cells.

Accumulation of zinc in intracellular fraction and cell wall. Zn accumulation in yeast strains was analysed after an incubation period in MSM + Glu + zinc media. Cell breakage was performed to enable the quantification of zinc that was either located intracellularly or bound to the cell wall (Fig. 6).

Distribution analysis has shown that zinc found in the supernatant and cell wall did not exceed 27% and 31% respectively, while the content was highest in the intracellular fraction (between 50% and 82%) (Fig. 6). Intracellular fractions of *Rh. mucilaginosa* (EB39), *C. parapsilosis* (ECF42) and *W. sorbophila* (ECF12) strains contained almost 80% of this heavy metal, but the zinc concentration on cell wall was the smallest for these strains (9%, 6% and 11% respectively).

In Fig. 6B, the zinc content/cell is shown. While all strains were inoculated at the same cell density, following growth in zinc-containing media strains of *C. parapsilosis*

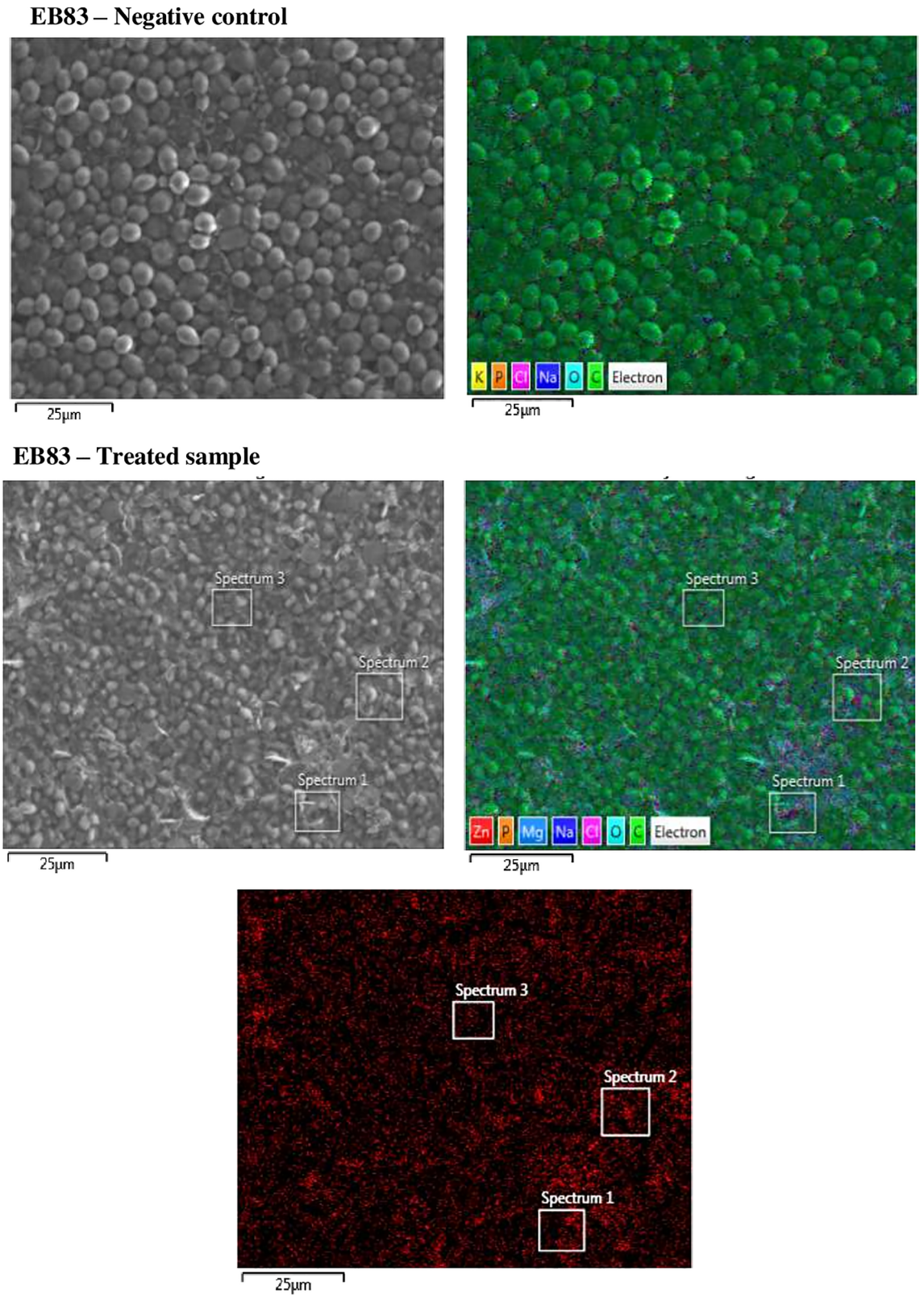

Fig. 5. Images generated by SEM-EDS of the strain EB83 (*S. cerevisiae*) treated and untreated (negative control). Black and white photos were taken just using the SEM for visualizing the samples, while those coloured show all the ion signals captured by the EDS coupled to the SEM. Red points identify Zn ions distributed in the sample (last image). [Color figure can be viewed at wileyonlinelibrary.com]

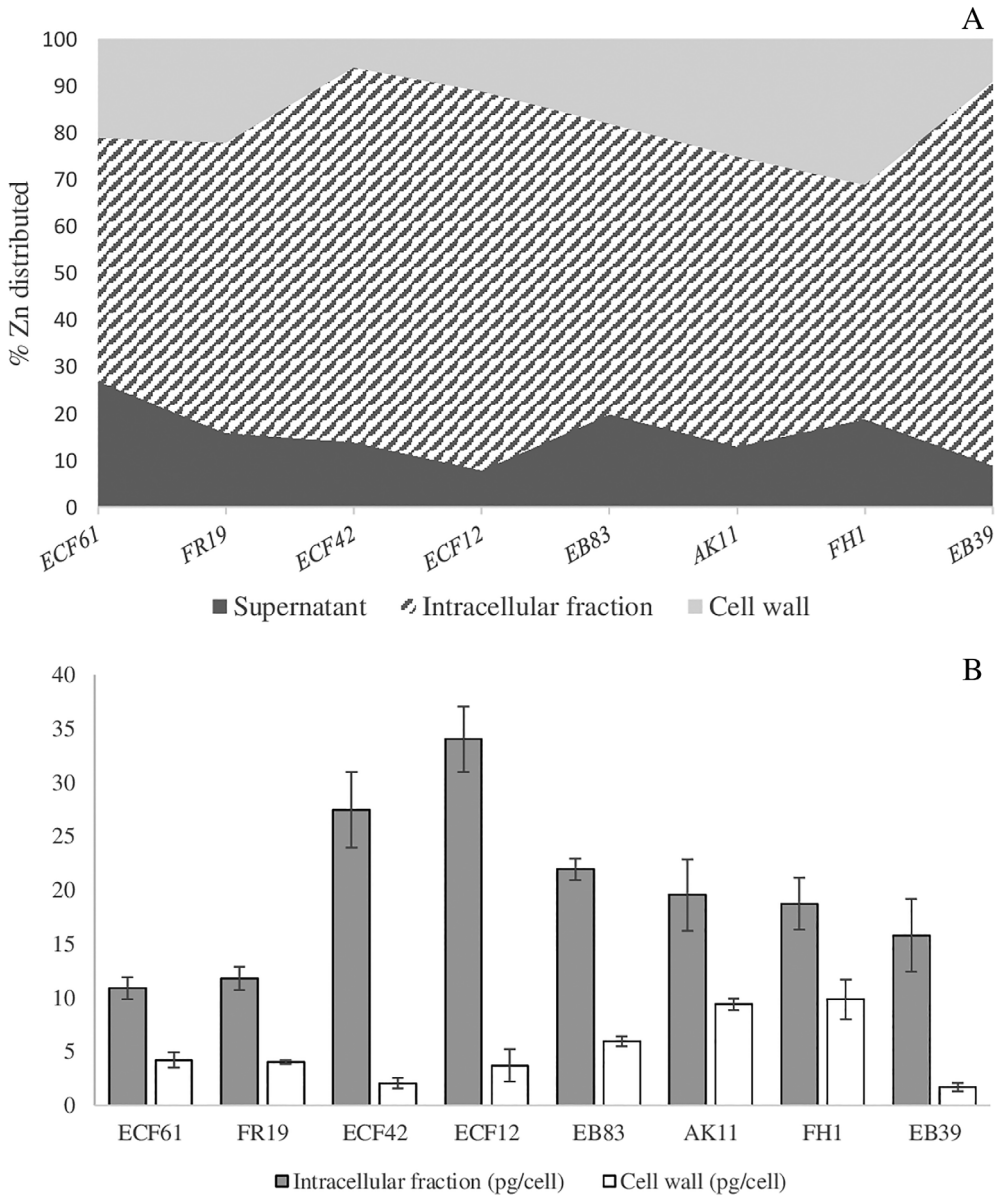

Fig. 6. (A) Zinc distribution (%) in cell parts and (B) its accumulation on intracellular fraction and cell wall per cell (pg/cell) in Saccharomyces and non-Saccharomyces strains after incubation (30°C/24 h) under Zn-replete conditions.

(ECF42) and *W. sorbophila* (ECF12) displayed the lowest cell counts and showed the highest zinc content in intracellular fractions (27.50 and 34 pg/cell respectively), while EB39 cell counts were around 10^7 cell ml^{-1} and zinc in the intracellular fraction was 21.97 pg/cell. In the rest of the strains, the highest zinc values were also found on the intracellular fractions, although the lowest content was found for ECF61 (*D. rugosa*) and FH1 (*A. pullulans*) (52% and 50% respectively) in comparison with the other strains.

With regard to the cell wall, *A. pullulans* (FH1) showed the highest zinc concentration, not only based on percentage distribution but also in the analysis per cell (9.88 pg/cell). A similar result was obtained for AK11 (*C. tropicalis*), 9.40 pg/cell on cell wall were quantified but distribution on whole cell indicated that 25% of Zn was found in cell wall while 62% was located in the intracellular fraction. The remaining strains, FR19 (*D. rugosa*) and EB83 (*S. cerevisiae*), showed the same Zn distribution in the intracellular fractions (62%) and very similar in the cell wall (22% and 18% respectively). Nevertheless, distribution per cells was completely different due to the high cell counts obtained for FR19 and ECF61 (*D. rugosa*) strains ($1.2–1.3 \times 10^7$ cells ml^{-1}).

Discussion

To the best of our knowledge, the proteomic response of yeast to zinc has been mainly investigated using *S. cerevisiae* as a model, with relatively few studies on non-model yeast. Therefore, it is important to survey responses to a variety of species under zinc-replete conditions. This study not only facilitates the identification of additional zinc-responsive proteins but also provides the first characterization of several non-*Saccharomyces* yeasts that have previously not been surveyed at a proteome level.

In this study, different effects were observed in the proteome of the strains tested under the same zinc-replete conditions at 25 mg/L. The proteome of strains ECF12 (*W. sorbophila*) and ECF42 (*C. parapsilosis*) did not show significant changes in response to zinc treatment which may indicate that they possess a different sensitivity to zinc at that concentration. Following incubation in Zn-replete conditions, these species showed a lower cell number than comparator species, and an associated higher Zn accumulation, which may lead to increased toxicity. Zinc oxide is known to have an antifungal effect against some *Candida* sp. (Souza *et al*., 2020) and, as Romero-Gil *et al*. (2016) documented, zinc salts interfered with cell growth of a yeast cocktail. Nonetheless, the percentage of the proteome modified in the remaining strains varied between 15% and 43.7%. Diverse transcriptomic and proteomic studies have been carried out using different zinc concentrations under replete conditions (10 μM and 3 mM—Lyons *et al*., 2000; 30 μM—de Curcio *et al*., 2017; 200 μM—Ehrensberger *et al*., 2013) which demonstrated zinc associated changes to the proteome of *S. cerevisiae*, *Schizosaccharomyces pombe* and *Paracoccidioides lutzii* respectively. These studies individually profile the molecular changes in these species using different concentrations of zinc in each case. To date, no investigations have yet compared various species or strains under the same zinc-replete conditions.

Quantitative and qualitative proteomic analysis of zinc-replete samples compared to zinc-depleted controls revealed common changes in levels of enzymes such as transferases, oxido-reductases and energy generation enzymes, as well as ion transmembrane transport and metal ion binding proteins. However, significant alterations in proteins related to other molecular functions were observed in each strain separately, highlighting distinct responses among the different strains. It is known that zinc is an ion with catalytic and structural functions as a protein cofactor, and that could be the reason why altered levels of enzymes have been detected in response to zinc (Maret, 2013). Additionally, the response of the two strains from the same species (FR19 and ECF61—*D. rugosa*) has revealed slight differences in the proteome alteration in response to zinc-replete conditions, which may allow us to distinguish some strain-specific responses that exist alongside the core proteins that show common alterations within the species.

Zinc-replete conditions seem to modulate the production of oxidoreductases, as described ahead and as documented previously (Wang *et al*., 2018), possibly due to the role of zinc as a structural constituent and as a cofactor. Alcohol dehydrogenases (Adh) are oxidoreductases that are associated with metal ion binding and zinc homeostasis (Vallee and Hoch, 1995; *Saccharomyces* genome database, 2000) and were characterized in all strains. These enzymes were elevated significantly in AK11 (*C. tropicalis*), ECF61 and FR19 (*D. rugosa*); in contrast to FH1 (*A. pullulans*) and EB39 (*Rh. mucilaginosa*) where they were decreased in abundance. Adh described in *S. cerevisiae*, mainly Adh1p are high abundance proteins and have two active sites for zinc in each monomer, therefore requiring a large amount of intracellular zinc (Lyons *et al*., 2000). It has been documented that under zinc-depleted conditions, all Adh proteins, except Adh4, can be seen to decrease in abundance with the aim of releasing trapped zinc for cell storage or for use in basic metabolic pathways (Wang *et al*., 2018). The increment in the number of these proteins may indicate that under zinc-replete conditions some strains overexpress them in order to capture zinc ions (Eide, 2009). However, Adh decreasing in other strains may indicate that an excess of zinc exists and mechanisms of homeostasis could maintain the zinc content at tolerable levels (Wang *et al*., 2018) or for the concentration used the strain is still capturing this metal ion, although further investigation would be required to confirm this aspect. Additionally, SOD and other oxidoreductases were elevated under these conditions but only SOD enzymes have been identified as proteins with known and potential structural zinc sites (Regalla and Lyons, 2005).

The elevation in the abundance of proteins related with energy generation process (ATPases, carbohydrates catalysis enzymes) and cellular reproduction (helicases, polymerases, ribosomal proteins) in some of the strains indicate that there is a restoration of normal growth in the zinc-replete samples, although helicase generation has been related previously with metal stress (Owttrim, 2006). Additionally, zinc-replete conditions seem to affect the normal function of another iron homeostasis in strains ECF61 and FR19 (*D. rugosa*) owing to the effect of high zinc levels on yeast cells has been previously related with the alteration of the assembly or function of iron–sulphur-containing proteins which are essential in the correct regulation of the iron homeostasis (Pagani *et al*., 2007).

Ribosome, mitochondria and Golgi apparatus were identified as relevant cellular component terms among the proteins with altered abundance under zinc-replete conditions in the eight strains tested. It is known that ribosomes contain zinc finger domains, mitochondria contain many metabolic enzymes (Regalla and Lyons, 2005) and Golgi apparatus contains zinc-dependent proteins for the secretory pathways and this ion is fundamental for its function (Ellis *et al*., 2004; Wu *et al*., 2011). Zinc deficiency leads to the downregulation of zinc-dependent ribosomal subunits which can also correspond with reduced growth rate, so the increase in these proteins in zinc-replete cells may indicate that cell growth rate is enhanced by this concentration of zinc in some strains (de la Cruz *et al*., 2018; Wang *et al*., 2018). Of the strains tested, FH1 (*A*. *pullulans*) was unique in that constituent proteins of the cell membrane were significantly increased. Moreover, a significant increase in transmembrane transport proteins ($p < 0.03$) and zf-ZPR1-domain-containing protein in response to zinc was observed (Li *et al*., 2019; Zeng *et al*., 2019). So that could indicate that this strain would tolerate and bind more zinc ions or that this strain exhibits an alternative response to zinc.

In zinc-depleted conditions, the expression of the ion transmembrane transporters is increased by Zap1 (Wang *et al*., 2018). In line with this, there was a significant decrease in ion transmembrane transporters, from the cell membrane and/or from vacuole, except for FH1 (*A*. *pullulans*) and EB39 (*Rh*. *mucilaginosa*), which is indicative of zinc sufficiency for some strains in the intracellular and vacuole space. Zap1-mediated regulation of zinc homeostasis has been characterized in *S*. *cerevisiae*, and other yeast species like *C*. *albicans* (Wilson and Bird, 2016), but it is unknown if similar mechanisms operate in other non-model yeast strains, such as those used in this study. The analysis of *S*. *cerevisiae* Zap1-regulated proteins was conducted to determine if analogous regulation takes place in the non-model yeast in response to zinc status. In line with previous studies, several Zap-1-regulated proteins were observed at lower abundance in the zinc-replete condition in *S*. *cerevisiae* (EB83) while some orthologous proteins (HSP12, cerevisin, saccharopepsin and others) were also at reduced levels in the non-*Saccharomyces* strains, indicating some features in common with *S*. *cerevisiae* zinc homeostasis in these strains (ECF61 and EB39). However, some orthologues of *S*. *cerevisiae* Zap1-regulated proteins showed opposing abundance changes to those observed in *S*. *cerevisiae* (cysteine proteinase 1, Adh1, Adh4…etc.) which might indicate other zinc homeostasis mechanisms could be operating in these strains, especially in *A*. *pullulans* (FH1) and *C*. *tropicalis* (AK11). These strains and proteins are candidates for future investigations on mechanisms of zinc homeostasis in yeast.

Based on the proteomic analysis, it has been observed that homeostasis mechanisms of the yeast strains studied may be the key factor in zinc elimination or bioaccumulation on the cell of this metal ion. This has allowed us to better understand which proteins and organelles are involved in this process as well as which strains showed a better response to zinc bioaccumulation.

Regarding zinc distribution in yeast, cell walls did not play a predominant role in zinc localisation, while the intracellular fraction (cytoplasm plus organelles) were the principal storage space in all strains analysed, as previous studies indicated (Simm *et al*., 2007; de Nicola and Walker, 2009). The small zinc content in the cell wall could be due to the fact that the adsorption mechanism might not be the principal way of zinc ion capture, and the principal function of the cell wall in zinc storing may be transporting the ions. However, FH1 (*A*. *pullulans*) had the highest percentage of zinc accumulated on the cell wall and protein constituents of the cell membrane were increased in abundance in FH1, thus an adsorption mechanism for zinc uptake may be used in some species. It was observed that the amount of zinc that yeast can accumulate depends on the species and is limited, never exceeding 35 pg/cell. In Simm *et al*. (2007) study, a limit of 0.06 pg vacuolar zinc/cell was established for *S*. *cerevisiae* in a media supplied with 100 μM $ZnCl_2$, so extracellular zinc concentration may alter the amount of zinc intracellular content. Moreover, de Nicola and Walker (2009) showed that zinc accumulation can vary depending on internal and external cell factors which can explain the different distribution observed by strain. Zinc distribution was also visualized by SEM-EDS and it was confirmed that cells at that concentration of this heavy metal may suffer stress, and cellular damage was detected in some strains. Moreover, it was found that zinc distribution was not homogeneous across all of the strains tested, which in turn is reflected by the differences observed in the proteomic response.

Conclusions

In this research, the proteome response and zinc distribution of eight strains from *Saccharomyces* and non-*Saccharomyces* yeast have been investigated under zinc-replete conditions. Proteomic analyses surveying 2000–3000 proteins from each strain have identified altered abundance, showing distinct profiles across the range of species tested. It was also observed that under zinc-replete conditions functional categories common to several strains showed altered abundance, such as transferases, oxido-reductases, growth-related proteins, ion transmembrane transport and metal ion binding proteins. In addition, specific changes have been observed in each strain highlighting the importance of extending

the analysis of zinc homeostasis to a range of non-model yeast. Adh has been detected to be relevant in certain strains for zinc ion binding while in other transmembrane transporters and zinc finger proteins were the ones implicated in this process. Moreover, the analysis of orthologues of Zap1-regulated proteins has allowed a comparison between zinc homeostasis mechanisms used by *S*. *cerevisiae* and the non-model strains. Zinc distribution analysis identified the intracellular fraction (cytoplasm plus organelles) as the principal storage part of the yeast cell, except in the case of FH1 (*A*. *pullulans*), and also demonstrated zinc distribution is not homogeneous across all yeast species. Nevertheless, more research needs to be carried out in this field in order to get more information and to fully characterize zinc homeostasis in each strain and this study will serve as a crucial foundation for future investigations.

Acknowledgements

Authors would like to thank Mr. Eduardo Prado García-Consuegra for his help and valuable knowledge in the SEM-EDS analysis.

Funding

This work was supported by the Castilla-La Mancha Regional Government, the European Social Fund and the Youth Employment Initiative (in line with the objectives of the RIS3) to BGB. Quantitative mass spectrometry facilities were funded by a competitive infrastructure award from Science Foundation Ireland [12/RI/2346 (3)].

References

Ayangbenro, A.S., and Babalola, O.O. (2017) A new strategy for heavy metal polluted environments: a review of microbial biosorbents. *Int J Environ Res Public Health* **14**: 94.

Chung, H., and Bird, A.J. (2019) Zinc signal in biology. In *Zinc Signalling*, Fukada, T., and Kambe, T. (eds). Singapore: Springer, pp. 389–410.

Collins, C., Hurley, R., Almutlaqah, N., O'Keeffe, G., Keane, T.M., Fitzpatrick, D.A., and Owens, R.A. (2017) Proteomic characterization of *Armillaria mellea* reveals oxidative stress response mechanisms and altered secondary metabolism profiles. *Microorganisms* **5**: E60.

Cox, J., and Mann, M. (2008) MaxQuant enables high peptide identification rates, individualized p.p.b.-range mass accuracies and proteome-wide protein quantification. *Nat Biotechnol* **26**: 1367–1372.

de Curcio, J.S., Silva, M.G., Silva Bailão, M.G., Báo, S.N., Casaletti, L., Bailão, A.M., and de Almeida Soares, C.M. (2017) Identification of membrane proteome of *Paracoccidioides lutzii* and its regulation by zinc. *Future Sci OA* **3**: FSO232.

de la Cruz, J., Gomez-Herreros, F., Rodriguez-Galan, O., Begley, V., de la Cruz Munoz-Centeno, M., and Chavez, S. (2018) Feedback regulation of ribosome assembly. *Curr Genet* **64**: 393–404.

de Nicola, R., and Walker, G.M. (2009) Accumulation and cellular distribution of zinc by brewing yeast. *Enzyme Microbial Technol* **44**: 210–216.

Delgado, J., Núñez, F., Asensio, M.A., and Owens, R.A. (2019) Quantitative proteomic profiling of ochratoxin A repression in *Penicillium nordicum* by protective cultures. *Int J Food Microbiol* **305**: 108243.

Ehrensberger, K.M., Mason, C., Corkins, M.E., Anderson, C., Dutrow, N., Cairns, B.R., *et al*. (2013) Zinc-dependent regulation of the Adh1 antisense transcript in fission yeast. *J Biol Chem* **288**: 759–769.

Eide, D.J. (2006) Zinc transporters and the cellular trafficking of zinc. *Biochim Biophys Acta* **1763**: 711–722.

Eide, D.J. (2009) Homeostatic and adaptive responses to zinc deficiency in *Saccharomyces cerevisiae*. *J Biol Chem* **284**: 18565–18569.

Ellis, C.D., MacDiarmid, C.W., and Eide, D.J. (2005) Heteromeric protein complexes mediate zinc transport into the secretory pathway of eukaryotic cells. *J Biol Chem* **280**: 28811–28818.

Ellis, C.D., Wang, F., MacDiarmid, C.W., Clark, S., Lyons, T., and Eide, D.J. (2004) Zinc and the Msc2 zinc transporter protein are required for endoplasmic reticulum function. *J Cell Biol* **166**: 325–335.

García-Béjar, B., Arévalo-Villena, M., Guisantes-Batan, E., Rodríguez, J., and Briones, A. (2020) Study of the bioremediatory capacity of wild yeasts. *Sci Rep* **10**: 11265. https://doi.org/10.1038/s41598-020-68154-4

Ghaemmaghami, S., Huh, W.K., Bower, K., Howson, R.W., Belle, A., Dephoure, N., *et al*. (2003) Global analysis of protein expression in yeast. *Nature* **425**: 737–741.

Kriventseva, E.V., Kuznetsov, D., Tegenfeldt, F., Manni, M., Dias, R., Simão, F.A., and Zdobnov, E.M. (2018) OrthoDB v10: sampling the diversity of animal, plant, fungal, protist, bacterial and viral genomes for evolutionary and functional annotations of orthologs. *Nucleic Acids Res* **47**: D807–D811.

Li, R., Miao, Y., Yuan, S., Li, Y., Wu, Z., and Weng, P. (2019) Integrated transcriptomic and proteomic analysis of the ethanol stress response in *Saccharomyces cerevisiae* Sc131. *J Proteomics* **203**: 103377.

Luber, C.A., Cox, J., Lauterbach, H., Fancke, B., Selbach, M., Tschopp, J., *et al*. (2010) Quantitative proteomics reveals subset-specific viral recognition in dendritic cells. *Immunity* **32**: 279–289.

Lyons, T.J., Gasch, A.P., Gaither, L.A., Botstein, D., Brown, P.O., and Eide, D.J. (2000) Genome-wide characterization of the Zap1p zinc-responsive regulon in yeast. *Proc. Natl. Acad. Sci. U. S. A.* **97**: 7957–7962.

MacPherson, S., Larochelle, M., and Turcotte, B. (2006) A fungal family of transcriptional regulators: the zinc cluster proteins. *Microbiol Mol Biol Rev* **70**: 583–604.

Maret, W. (2013) Zinc biochemistry: from a single zinc enzyme to a key element of life. *Adv Nutr* **4**: 82–91.

Owttrim, G.W. (2006) RNA helicases and abiotic stress. *Nucleic Acid Res* **34**: 3220–3230.

Pagani, M.A., Casamayor, A., Serrano, R., Atrian, S., and Ariño, J. (2007) Disruption of iron homeostasis in *Saccharomyces cerevisiae* by high zinc levels: a genome-wide study. *Mol Microbiol* **65**: 521–537.

Regalla, L.M., and Lyons, T.J. (2005) Zinc in yeast: mechanisms involved in homeostasis. In *Molecular Biology of Metal Homeostasis and Detoxification. Topics in Current Genetics*, Tamas, M.J., and Martinoia, E. (eds). Berlin: Springer, pp. 37–58.

Romero-Gil, V., Rejano-Zapata, L., Garrido-Fernández, A., and Arroyo-López, F.N. (2016) Effect of zinc formulations, sodium chloride, and hydroxytyrosol on the growth/no-growth boundaries of table olive related yeasts. *Food Microbiol* **57**: 71–80.

Saleh, A.A., Jones, G.W., Tinley, F.C., Delaney, S.F., Alabbadi, S.H., Fenlon, K., *et al*. (2018) Systems impact of zinc chelation by the epipolythiodioxopiperazine dithiol gliotoxin in *Aspergillus fumigatus*: a new direction in natural product functionality. *Metallomics* **10**: 854–866.

Simm, C., Lahner, B., Salt, D., LeFurgey, A., Ingram, P., Yandell, B., and Eide, D.J. (2007) *Saccharomyces cerevisiae* vacuole in zinc storage and intracellular zinc distribution. *Eukaryot Cell* **6**: 1166–1177.

Souza, J., Araujo, A., Carvalho, A., Amorim, A., Daboit, T., Leite, J., *et al*. (2020) Sustainably produced cashew gum-capped zinc oxide nanoparticles show antifungal activity against *Candida parapsilosis*. *J Clean Prod* **247**: 119085.

Tchounwou, P.B., Yedjou, C.G., Patlolla, A.K., and Sutton, D.J. (2012) Heavy metals toxicity and the environment. *EXS* **101**: 133–164.

Tyanova, S., Temu, T., Sinitcyn, P., Carlson, A., Hein, M.Y., Geiger, T., *et al*. (2016) The Perseus computational platform for comprehensive analysis of (prote)omics data. *Nat Methods* **13**: 731–740.

Vallee, B.L., and Hoch, F.L. (1995) Zinc, a component of yeast alcohol dehydrogenase. *Proc Natl Acad Sci U S A* **41**: 327–338.

Wang, Y., Weisenhorn, E., MacDiarmid, C.W., Andreini, C., Bucci, M., Taggart, J., *et al*. (2018) The cellular economy of the *Saccharomyces cerevisiae* zinc proteome. *Metallomics* **10**: 1755–1776.

Wilson, S., and Bird, A.J. (2016) Zinc sensing and regulation in yeast model systems. *Arch Biochem Biophys* **611**: 30–36.

Wu, Y.H., Frey, A.G., and Eide, D.J. (2011) Regulation of the Zrg17 zinc transporter in the yeast secretory pathway. *Biochem J* **435**: 259–266.

Zeng, H., Zhang, X., Ding, M., and Zhu, Y. (2019) Integrated analyses of miRNAome and transcriptome reveal zinc deficiency responses in rice seedlings. *BMC Plant Biol* **19**: 585.

Zhao, X.Q., and Bai, F.W. (2012) Zinc and yeast stress tolerance: micronutrient plays a big role. *J Biotechnol* **158**: 176–183.

Supporting Information

Additional Supporting Information may be found in the online version of this article at the publisher's web-site:

Figure S1. Images generated by SEM-EDS of the non-model strains treated and untreated (negative control). Black and white photos were taken just using the SEM for visualizing the samples, while those coloured show all the ion signals captured by the EDS coupled to the SEM. Red points identify Zn ions distributed in the sample (last image).

Supplementary Table 1. Strain information: Origin, isolation date and protein database.

Supplementary Table 2. *S. cerevisiae* and non-model yeast proteins identified in this study along with log2 (fold change) and significance values (p) of Zn+ compared with Zn− conditions.

Supplementary Table 3. Functional enrichment analysis of proteins that increased or decreased in abundance in the 8 yeast strains tested in response to zinc presence. Significantly enriched GO terms are indicated ($p < 0.05$).

Supplementary Table 4. Functional identification of metal ion binding proteins obtained by Blas2Go analysis.

Supplementary Table 5. Abundance change of Zap1-regulated zinc responsive *S. cerevisiae* proteins and their orthologs found in the non-*Saccharomyces* strains tested. Proteins that decreased abundance in Zn+ compared to Zn− samples are marked in green and proteins that increased abundance in Zn+ compared to Zn− samples in red.